archives
of thermodynamics
Vol. **33**(2012), No. 4, 41–65
DOI: 10.2478/v10173-012-0027-7

Thermodynamic analysis of biofuels as fuels for high temperature fuel cells

JAROSŁAW MILEWSKI*
WOJCIECH BUJALSKI
JANUSZ LEWANDOWSKI

Institute of Heat Engineering, Warsaw University of Technology,
00-665 Warsaw, Nowowiejska 21/25, Poland

Abstract Based on mathematical modeling and numerical simulations, applicativity of various biofuels on high temperature fuel cell performance are presented. Governing equations of high temperature fuel cell modeling are given. Adequate simulators of both solid oxide fuel cell (SOFC) and molten carbonate fuel cell (MCFC) have been done and described. Performance of these fuel cells with different biofuels is shown. Some characteristics are given and described. Advantages and disadvantages of various biofuels from the system performance point of view are pointed out. An analysis of various biofuels as potential fuels for SOFC and MCFC is presented. The results are compared with both methane and hydrogen as the reference fuels. The biofuels are characterized by both lower efficiency and lower fuel utilization factors compared with methane. The presented results are based on a 0D mathematical model in the design point calculation. The governing equations of the model are also presented. Technical and financial analysis of high temperature fuel cells (SOFC and MCFC) are shown. High temperature fuel cells can be fed by biofuels like: biogas, bioethanol, and biomethanol. Operational costs and possible incomes of those installation types were estimated and analyzed. A comparison against classic power generation units is shown. A basic indicator net present value (NPV) for projects was estimated and commented.

Keywords: Solid oxide fuel cell; Molten carbonate fuel cell; Mathematical modeling; Biofuels

*E-mail address: milewski@itc.pw.edu.pl

1 Introduction

Fuel price inflation and a long-term increase in electricity consumption have provided added impetus to the search for ultra-effective power generation systems. Fuel cells generate power in electrochemical reactions with potentially ultra-high efficiency. High temperature fuel cells (mainly solid oxide fuel cell (SOFC) and molten carnonate fuel cell (MCFC) are considered as future electricity sources. Presently, the state-of-the-art hybrid systems including SOFC and MCFC are being built in the 250 kW power range. Research and development in this field is predicted to result in the increase in power of those kinds of systems in the future.

Hydrogen and methane (in the form of natural gas) are currently considered to be the main fuels for fuel cells. Hydrogen is an ideal fuel with respect to fuel cell working conditions. Unfortunately, hydrogen is not present in the environment in an uncombined form and there are difficulties with production, transportation and storage. Methane, meanwhile, is considered to be the interim fuel due to limited resources.

The most plausible future scenarios in the power markets are as follows:

1. Abandoning gas/liquid/solid fuels in favour of electricity generated by renewable sources and/or nuclear plants. In this case, the energy distribution role will be provided by the power grid, and the storage role by consumers.

2. Production of plant-derived gas/liquid fuels based on the cultivation of plants and shrubs, such as Salix viminalis, and their conversion into fuel, e.g., alcohols.

Using electricity only can be problematic (e.g., airplanes), the cultivation of 'energy' seems to be one of the most possible scenarios for the future. So then, one of the most plausible future scenarios in the power markets is the production of plant-derived gas/liquid fuels based on the cultivation of plants and shrubs, such as Salix viminalis, and their conversion into fuel, e.g., alcohols. The advantages of this approach include: easy storage, existing distribution network, easiness to implement in the transport industry (especially in airplanes) and potential eco-friendly aspects. Hydrogen and methane are considered as fuels for fuel cells at present. The use of biogas in fuel cells is relatively poorly investigated. Some data can be found in [1–3]. Most developments regard singular cell tolerance on impurities or biogas content. Mainly, the investigations are focused on biogas taken

from sewage treatment plants or gasifiers. In many cases the biogas is first reformed to hydrogen and then hydrogen is delivered to the cell.

2 Biofuels

Biofuel is defined as a solid, liquid or gaseous fuel obtained from relatively recently lifeless or living biological material and it differs from the fossil fuels, which are derived from the biological material stored underground for a long time. The use of biogas in fuel cells has been relatively poorly investigated. Some data can be found in [1–3]. The presented analysis considers biofuels obtained from biomass gasification as well as fermentation processes. Taken into consideration were the following biofuels: biogases (anaerobic digester gas – ADG, landfill gas – LFG); bioliquids (methanol, ethanol, canola oil); solids – wood. Hydrogen and methane were used as reference fuels.

Anaerobic digestion is a series of processes in which microorganisms break down biodegradable material in the absence of oxygen. The presented analysis considers ADG produced by wastewater treatment plants. Landfill gas is produced by wet organic waste fermentation under anaerobic conditions in a landfill site. The waste is covered and compressed both mechanically and by the weight of the material that is deposited from above. This material prevents oxygen from accessing the waste thereby encouraging anaerobic microbes to thrive and produce gas, which slowly escapes and is captured. The composition of LFG and ADG are listed in Tab. 2. Those types of gases consist mainly of methane and carbon dioxide.

Table 1. Factors used for steam content calculations.

Biofuel	Factor name and reference	Definition (by molar fractions)	Value assumed during calculations
Biogases, Canola Oil Syngas, Wood Syngas	steam to carbon ratio [4] (s/c ratio)	H_2O/CH_4 +CO	1.4 (see Fig. 1)
Biomethanol	steam to methanol ratio [5]	H_2O/CH_3OH	1 (see Fig. 2)
Bioethanol	steam to ethanol ratio [6]	H_2O/C_2H_5OH	3 (see Fig. 3)

Canola is a cultivar of oilseed rape (*Brassica campestris*). Canola oil is considered as alternative fuel to diesel, and is termed the biodiesel. It is made by extracting oil from the seeds. Usually, the process takes place at

Table 2. Biogas composition (molar fractions).

Component	Landfill gas	Anaerobic digester gas
CH_4	54%	63%
CO_2	33%	35%
Other	13%	2.0%
Initial s/c ratio	0.15	0.02

elevated temperatures. The canola oil consists mainly of long-chain hydrocarbon fatty acids (see Tab. 3).

Table 3. Canola oil composition.

Component	Chemical structure	Molar fraction [%]
Oleic acid	CH_3-$(CH_2)_7$-CH=CH-$(CH_2)_7$-COOH	75
Linoleic acid	CH_3-$(CH_2)_4$-CH=CH-CH_2-CH=CH-$(CH_2)_7$-COOH	15
α-Linolenic acid	CH_3-CH2-CH=CH-CH_2-CH=CH-CH_2-CH=CH-$(CH_2)_7$-COOH	10

Wood is composed mainly of lignin, cellulose, and hemicelluloses (see Tab. 4). The structure of hemicelluloses is very similar to cellulose itself, so in the presented analysis it was assumed that the wood delivered to the gasifier consisted only of cellulose (75%) and lignin (25%).

Table 4. Wood composition

Component	Chemical structure	Molar fraction [%]
Cellulose	...-OH-CH_2-(CH-O)$_2$-(CH_2O)$_2$-CH-...	50
Hemicelluloses	...-OH-CH_2-(CH-O)$_2$-(CH_2O)$_2$-CH-...	24
Lignin	...-OH-CH_2-CH=CH-(CH=C)$_2$-OH-CH=C-CH_3O-...	23
Other components		3

For safe fuel cell operation, steam is added to carbon-containing fuels to prevent carbon deposition on the cell surfaces (see Tab. 1). Various kinds of factors are used to describe adequate steam content in hydrocarbon fuel to avoid carbon deposition. Carbon deposition is a harmful process that causes very rapid degradation of fuel cells and the reformer. For gaseous hydrocarbon fuel, the most commonly used factor is the steam-to-carbon

ratio (s/c ratio). Mostly, the s/c ratio is set at about 2 and above this value no carbon deposition takes place. Boundary values of the s/c ratio are dependent on temperature. Drawn from a review of the literature, typical factors and their definitions for various fuels are listed in Tab. 4. The s/c ratio at which no carbon deposition occurs is temperature dependent, as is shown in Fig. 1.

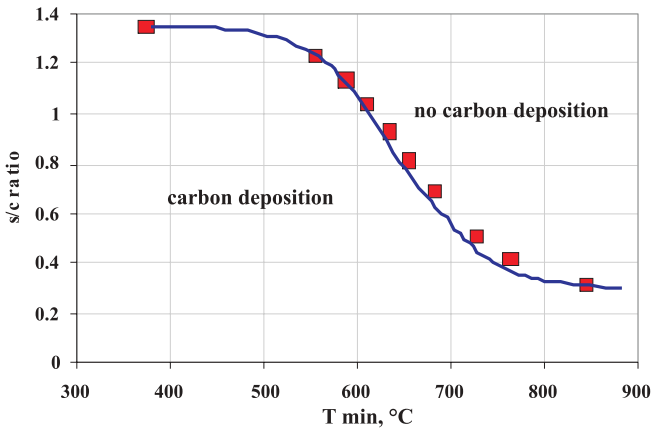

Figure 1. Minimum temperature and corresponding required ratios of steam-to-carbon (s/c) above which no carbon deposition occurs thermodynamically [4].

The steam addition to the fuel results in the following decomposition of water into hydrogen during the steam reforming reactions. The steam reforming reaction based on two reactions (reforming reaction):

$$CH_4 + H_2O \rightarrow 3H_2 + CO \tag{1}$$

and gas shift reaction:

$$CO + H_2O \leftrightarrow H_2 + CO_2\ . \tag{2}$$

Overall, the reactions (1) and (2) are endothermic, which means that thermal energy is used for water decomposition into hydrogen what results in conversion of heat into the form of fuel (mainly water decomposition into hydrogen). This means that fuel cell efficiency based on the calculation of chemical energy of the delivered fuel (without taking into account of delivered heat) can reach values of above 100% (e.g., in the case of carbon oxidization).

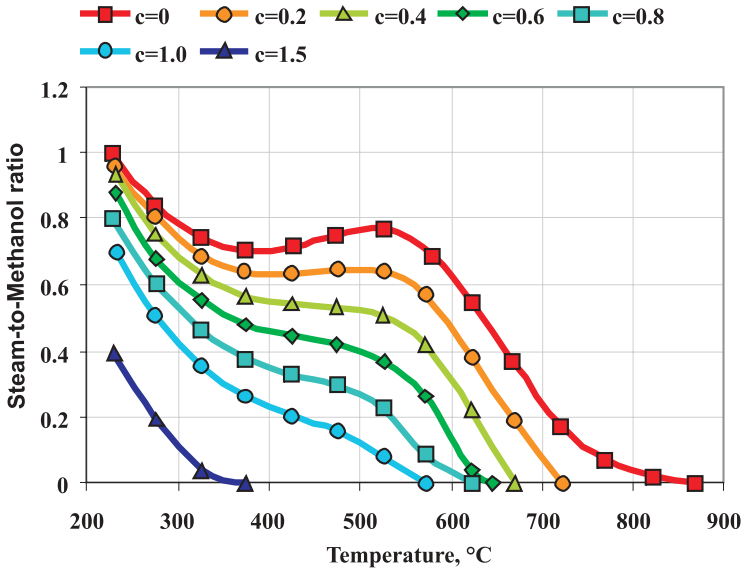

Figure 2. Minimum temperature and corresponding required ratios of steam-to-methanol (c/MeOH) above which no carbon deposition occurs [5]. The 'c' symbol means a fraction of carbon wich is deposited.

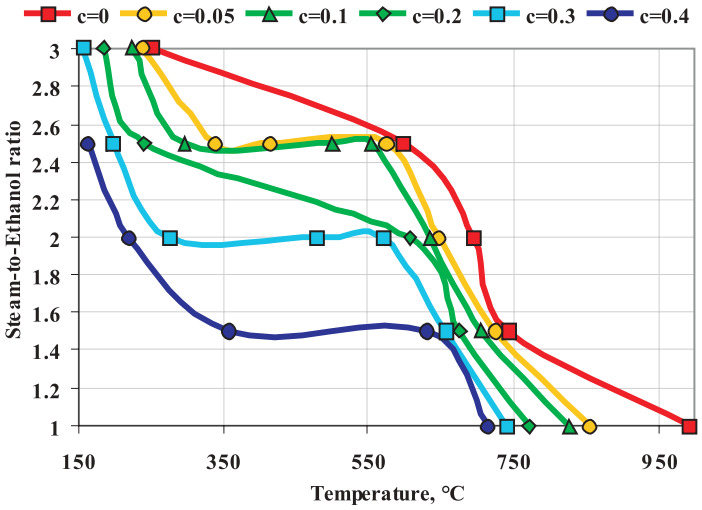

Figure 3. Minimum temperature and corresponding required ratios of steam-to-ethanol (S/EtOH) above which no carbon deposition occurs [6]. 'c' means a fraction of carbon wich is deposited.

3 Theory

The presented results are based on calculations made using an appropriate mathematical model [7]. Those calculations are based on the Lee-Kesler equation of state and minimization of Gibbs free energy [8]. The used software also calculates mass and energy balances in each point, thus is not necessary to present them in the paper.

The maximum voltage of the fuel cell depends on the type of reaction occurring on the electrode surfaces. Biogas in reaction with oxygen can give various maximum voltages. Mixtures of various components occur in the case of the analyzed fuels. The maximum values of voltage for various reactions are listed in Tab. 5.

Table 5. Temperature dependence of ionic conductivity for solid oxides.

Component	Chemical Reaction	Maximum Voltage, E_{max} [V]
H_2	$H_2 + 1/2O_2 \rightarrow H_2O$	1.23
CH_4	$CH_4 + 2O_2 \rightarrow CO_2 + H_2O$	1.06
CH_3OH	$CH_3OH + 3/2O_2 \rightarrow CO_2 + 2H_2O$	1.22
C	$C + O_2 \rightarrow CO_2$	1.03
C	$C + 1/2O_2 \rightarrow CO$	0.72
CO	$CO + 1/2O_2 \rightarrow CO_2$	1.34

3.1 Solid oxide fuel cell

The governing equations for the SOFC model are presented in this section. The presented analysis considers a design point estimation of the SOFC. This means that the value of maximum current density (I_{max}) is constant. In the present study, the I_{max} was assumed at the value of 2.6 A/cm^2. The fuel cell characteristic is defined by a voltage-current density curve ($E = f(I)$). In the case of design point calculations, the voltage-fuel utilization factor curve ($E = f(\eta_f)$) is the fuel cell characteristic. The other model assumptions are: anode inlet pressure = 0.1 MPa, cathode inlet pressure = 0.1 MPa, temperature = 800 °C.

The mixture of various hydrocarbons enters into the SOFC anode, so the fuel utilization factor is calculated based on the equivalent hydrogen molar flow. The equivalent hydrogen molar flow at the anode inlet is defined by

the following relationship:

$$n_{H_2,eq} = n_{H_2} + n_{CO} + 3n_{CH_3OH} + 4n_{CH_4} + 6n_{C_2H_5OH} + 7n_{C_2H_6} + 10n_{C_3H_8} + 13n_{C_4H_{13}} \tag{3}$$

where: n – molar flow at anode inlet; H_2 – hydrogen; CH_4 – methane; CH_3OH – methanol; C_2H_5OH – ethanol; C_2H_6 – ethane; C_3H_8 – butane; C_4H_{13} – propane.

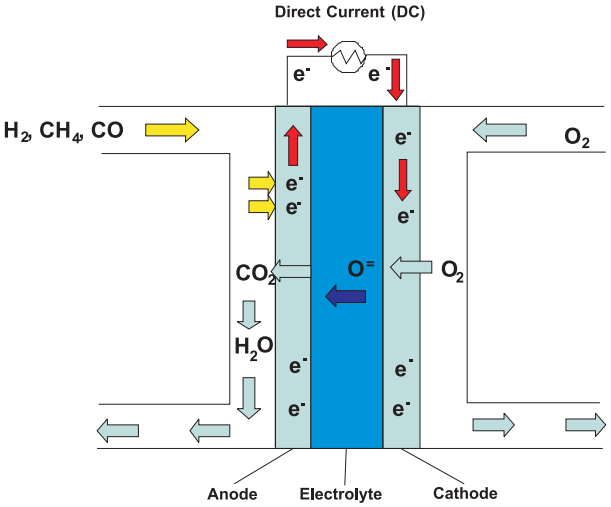

Figure 4. Working principles of SOFC.

Mixtures of various components occur in the case of the analyzed fuels. Due to these circumstances the general form of Nernst's equation is used to estimate the voltage of SOFC.

$$E_{\max} = \frac{RT}{4F} \ln \frac{p_{O_2,ca}}{p_{O_2,an}} \tag{4}$$

where: T – absolute temperature, R – universal gas constant, F – Faraday's constant, $p_{O2,ca}$ – oxygen partial pressure at cathode outlet, $p_{O2,an}$ – oxygen partial pressure at anode outlet. Adequate partial pressures were calculated through the use of simulation software HYSYS [8].

Based on working principles presented in Fig. 4, the equivalent electric circuit of a singular cell is shown in Fig. 5 [7].

Two types of resistance are present in fuel cells: ionic resistance R_1 and electric resistance R_2 (see Fig. 5). Resistance R_3 is the external load resistance of the fuel cell. Voltage generated by a singular cell is given by the

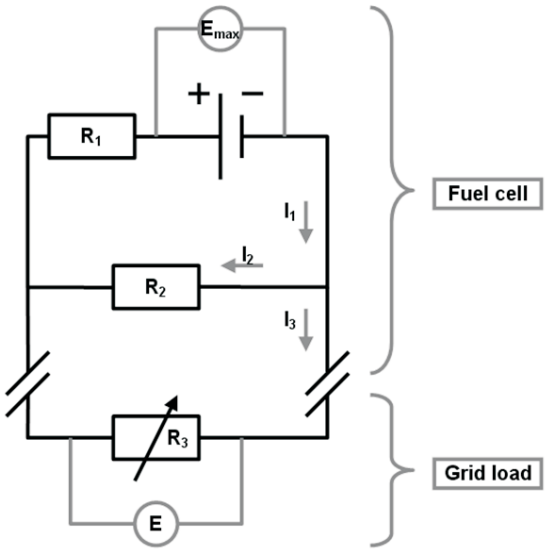

Figure 5. Equivalent electric circuit of the cell [7].

following equation [7,15–20]:

$$E_{SOFC} = \frac{E_{\max} - \eta_f I_{\max} R_1}{\frac{R_1}{R_2}(1-\eta_f)+1}\ , \tag{5}$$

where: E_{max} – maximum voltage; η_f – fuel utilization factor, I_{max} – maximum current density, R_1 – internal ionic area specific resistance of the cell, R_2 – internal electronic area specific resistance of the cell.

The second type of internal resistance is electric resistance – R_2 (see Fig. 5). The influences of temperature and electrolyte thickness on the electronic internal resistance of electrolytes are not well known. The electronic conductivity values of solid oxide electrolytes are probably spread across a very wide range. They do not have a major impact on calculated cell voltage for high fuel utilization factors. It is difficult to measure the electronic resistance of solid oxide electrolytes since they have both conductivities – ionic and electronic – simultaneously, which gives total electrical resistance. It should be noted that decreasing electrolyte thickness reduces ionic resistance, but also probably reduces electronic resistance.

The value of electronic resistance of the cell can be estimated from available experimental results. The value of 2.2 cm^2/S, was taken from

the authors own calculations, which were based on data presented in [9,10]. This value was assumed to be independent of temperature. The electrolyte was assumed at 30 μm. The I_{max} of 5.23 A/cm^2 was determined by the authors own calculations, which were based on data taken from [9,10].

The ionic resistance of solid oxides as a function of electrolyte temperature is shown in Fig. 6.

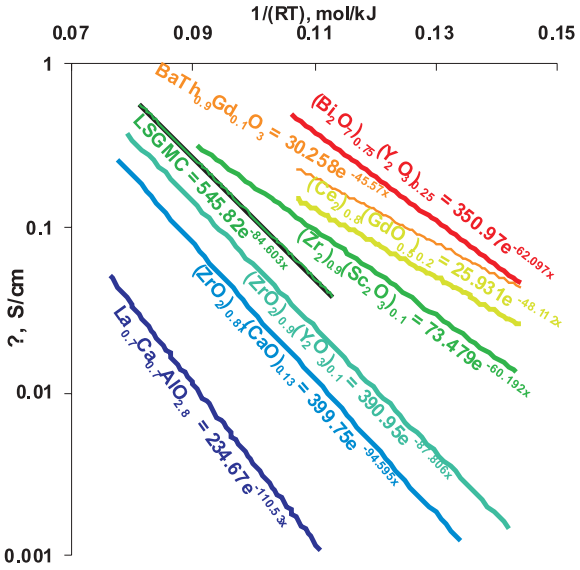

Figure 6. Temperature dependence of ionic conductivity for solid oxides.

The internal area specific ionic resistance can be described by the following relationship:

$$R_1 = \frac{\delta}{\sigma} \,, \tag{6}$$

where: δ – electrolyte thickness; σ – ionic conductivity of solid oxide. The ionic conductivity of the carbonate is defined as follows:

$$\sigma = \sigma_0 e^{\frac{-E}{RT}} \,, \tag{7}$$

where: σ_0 [S/cm], E [kJ/mol] – factors dependent on material used. The Yttrium stabilized zirconium (YSZ) was used as an electrolyte during the simulations. The factors σ_0 and E for this electrolyte are: 390.95S/cm and 87.806 kJ/mol, respectively (see Fig. 6).

The total current which can be drawn from the cell is strictly correlated with the amount of fuel delivered. This means that it is a value of current for which the whole fuel is utilized – I_{max}. Then, the fuel utilization factor can be correlated with the current generated by the cell

$$\eta_f = \frac{I}{I_{\max} - I_2} \,, \tag{8}$$

where: I – current density, I_{max} – maximum current density, I_2 – internal current density of the cell coused by internal electric resitance (R_2 – see Fig. 5).

$$I_{\max} = 2F\dot{n}_{H_2,eq} \,, \tag{9}$$

where $\dot{n}_{H2}$ is the energy equivalent molar flow of hydrogen.

The presented model was compared with experimental data; this comparison is shown in Fig. 7. The model was compared with experimental data for humidified hydrogen as a fuel diluted by helium [9]. The quantity of delivered oxidant (air) was adjusted to keep fuel cell temperature at assumed level. Average value of an oxidant utilization factor is 24%.

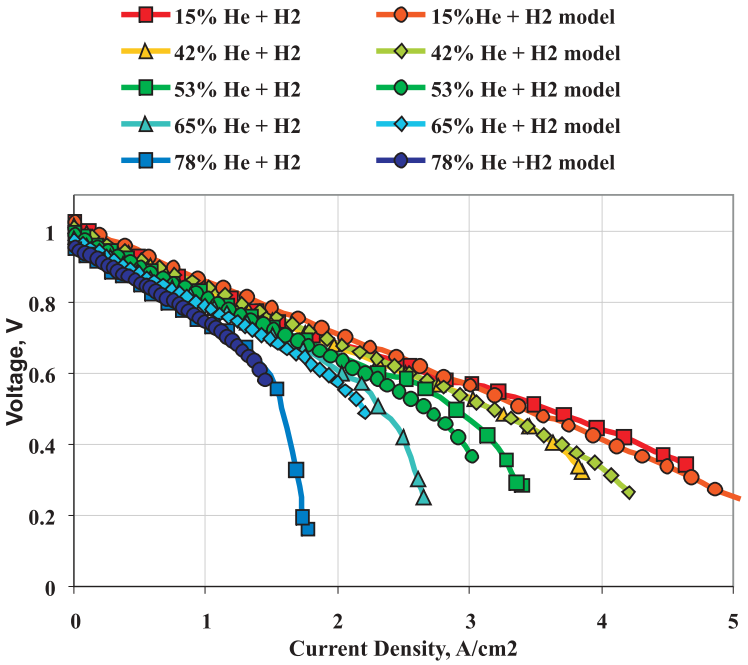

Figure 7. Experimental and simulations data at various H_2 molar fractions [9].

3.2 Molten carbonate fuel cell

The governing equations for the MCFC model are presented in this section. The presented analysis considers a design point estimation of the MCFC. This means that the value of maximum current density (I_{max}) is constant. In the present study the I_{max} was assumed at the value of 0.15 A/cm^2. The fuel cell characteristic is defined by a voltage-current density curve ($E = f(I)$). In the case of design point calculations the voltage-fuel utilization factor curve ($E = f(\eta_f)$) is the fuel cell characteristic. The other model assumptions are: anode inlet pressure = 0.1 MPa, cathode inlet pressure = 0.1 MPa, temperature = 650 °C. The mixture of various hydrocarbons enters into the MCFC anode, so the fuel utilization factor is calculated based on an equivalent hydrogen molar flow. The equivalent hydrogen molar flow at the anode inlet is defined by the following relationship (3).

The general form of Nernst's equation is used to estimate the voltage of MCFC.

$$E_{\max} = \frac{RT}{4F} \ln \frac{p_{O_2,ca} \cdot p^2_{CO_2,ca}}{p_{O_2,an} \cdot p^2_{CO_2,an}} \tag{10}$$

where: T – absolute temperature, R – universal gas constant, F – Faraday's constant, p – partial pressure, O_2 – oxygen, CO_2 – carbon dioxide. Adequate partial pressures were calculated through the use of HYSYS software [8].

The ionic resistance of molten carbonate electrolytes as a function of temperature is shown in Fig. 8. This diagram contains values obtained by authors own calculations, which were based on data published by Morita *et al.* [11]. It was assumed that the thickness of the Li/K electrolyte matrix was 1 mm. The I_{max} and R_2 value of 0.6 A/cm^2 and 28 Ωcm^2, respectively, were determined by authors own calculations (see Tab. 6), which were based on data provided by Arato et al. [12]. The results obtained for the presented model was compared with experimental data in Fig. 9.

3.3 Gasifier

Gasifier is calculated based on the minimum of Gibbs free energy of the mixture. Thermodynamic properties of the syngas are obtained through the use of the Peng-Robinson equation of state. Some types of biofuels cannot be delivered to the SOFC directly. In those cases, the gasifier was applied. The gasifier is fed simultaneously by oxygen and steam to achieve the autothermal process. For safe operation of the fuel cell, steam is added

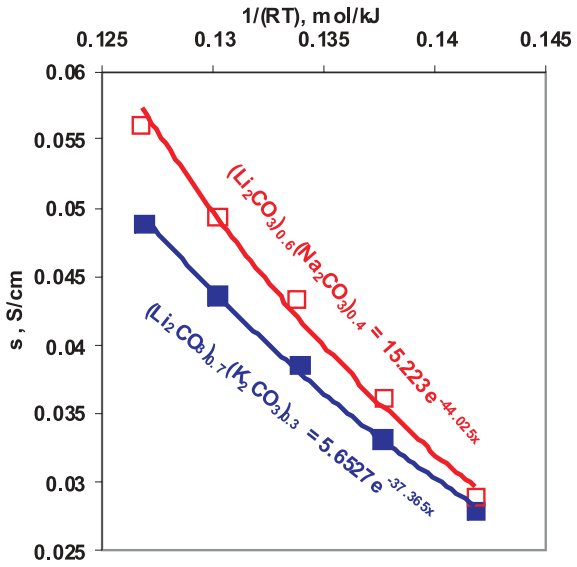

Figure 8. Temperature dependence of ionic conductivity for molten carbonates.

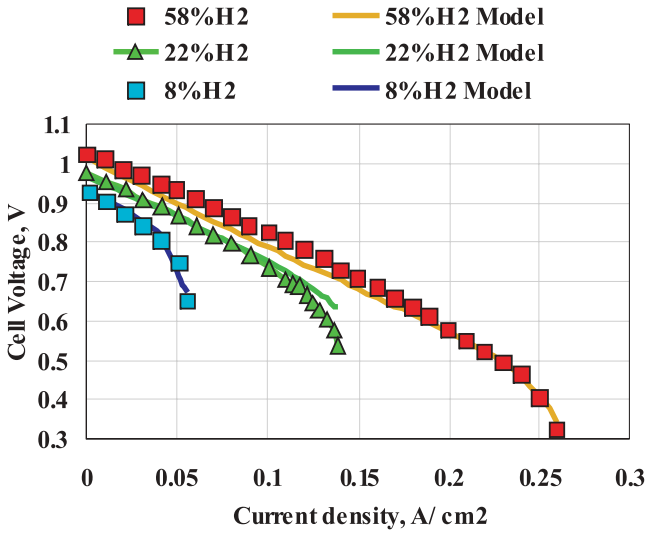

Figure 9. Experimental and simulations data at different H_2 molar fractions [12].

to carbon-containing fuels to prevent carbon deposition on the cell surfaces. The gasifier was modelled as an adiabatic unit and oxygen delivered to

Table 6. Fuel cell parameters used for the model validation.

Parameter	SOFC	MCFC
Maximum current density, I_{max}, A/cm^2	2.6	0.15
Temperature, °C	800	650
Pressure, MPa	1	1
Electronic resistance, R_2, cm^2/S	2.2	28
Electrolyte material	YSZ (see Fig. 6)	$LiCO_3/NaCO_3$ (see Fig. 8)
Electrolyte thickness, μm	15	1000

the gasifier in adequate quantity to maintain the assumed temperature. The gasifier model was created in the enviroment used software [8] and is presented in Fig. 10.

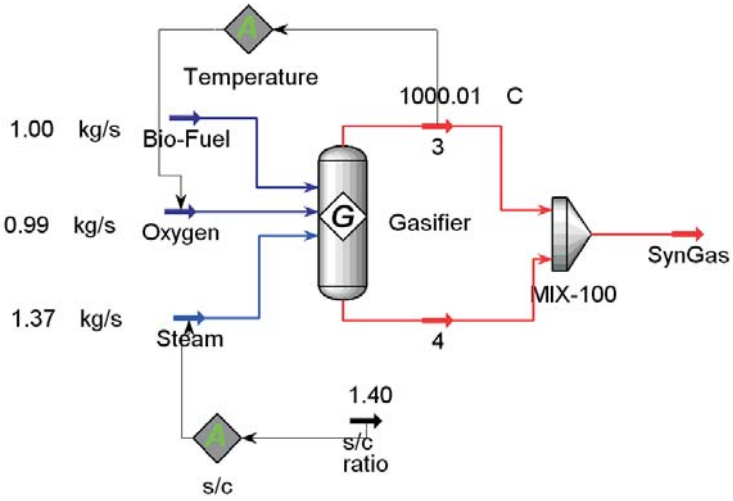

Figure 10. Gasifier model.

Using the model, the gasifier characteristics were generated for both fuels: canola oil and wood. The characteristics are presented in Figs. 11 and 12. The syngas obtained by biomass gasification is characterized by a high content of carbon monoxide (35%) and steam (30%) and a low content of hydrogen (5%). There is almost no methane in the syngas. A high inert gases content is also observed (carbon dioxide 35%), which decreases the higher heating value (HHV)of the syngas.

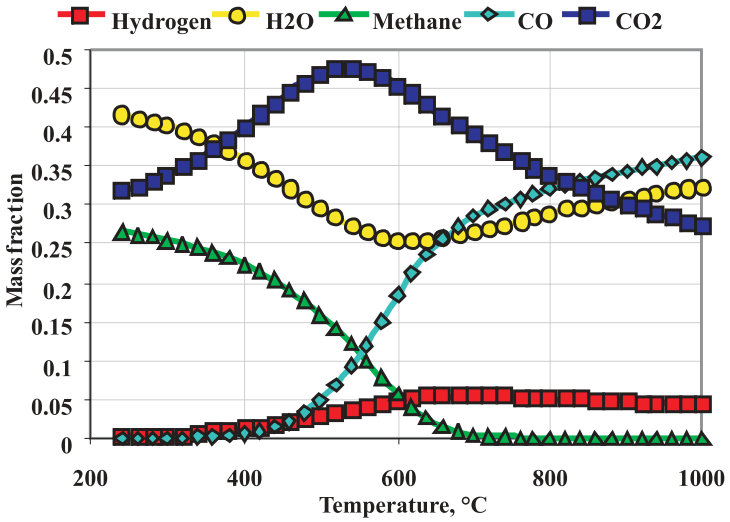

Figure 11. Canola oil syngas composition as a function of temperature.

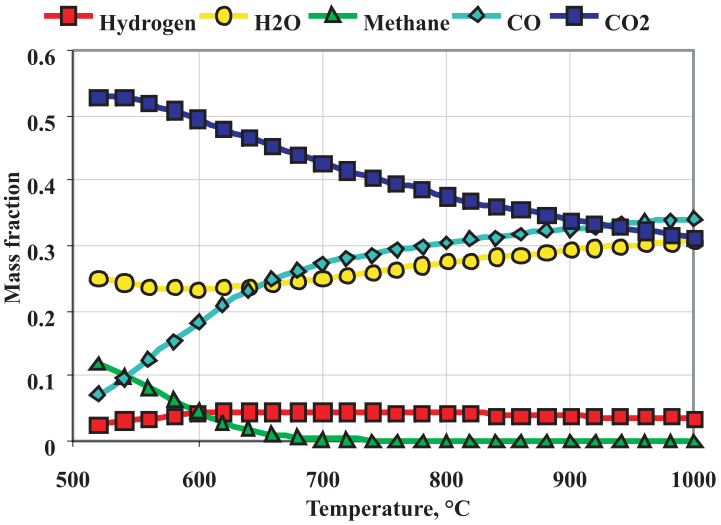

Figure 12. Wood syngas composition as a function of temperature.

4 Results and discussion

The main factor used to compare the systems is an efficiency defined by the following relationship:

$$\eta = \frac{EI_{\max}\eta_f A}{\dot{m}_{fuel} HHV_{fuel}}\,, \tag{11}$$

where: E – fuel cell voltage [V], I_{max} – fuel cell maximum current density [A/cm^2], η_f – fuel utilization factor, A – fuel cell active area [cm^2], $\dot{m}$ – fuel mass flow [kg/s], HHV – higher heating value of a fuel [kJ/kg].

4.1 Solid oxide fuel cell fuelled by biofuels

The SOFC voltages and obtained efficiencies for various fuels are shown in Figs. 13 and 14. The figures contain the cell voltages and efficiencies for various fuels as a function of the fuel utilization factor. The SOFC efficiency

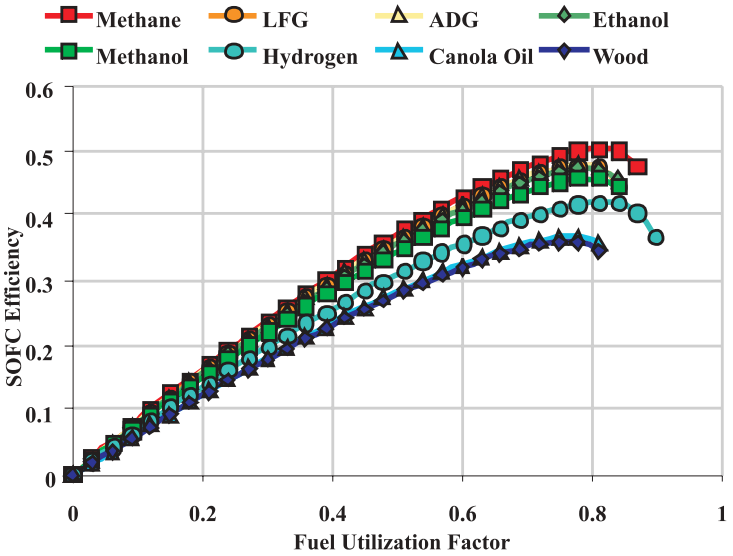

Figure 13. SOFC efficiency vs. fuel utilization factor for various biofuels.

curves are shown in Fig. 13, the highest values (50%) are obtained for methane as a fuel, syngases are characterized by much lower performances (35%). The highest optimum fuel utilization factor is for hydrogen as a fuel (80%) whereas the lowest one is for canola oil syngas (75%).

4.2 Molten carbonate fuel cells fuelled by biofuels

MCFC voltages and obtained efficiencies for various fuels are shown in Figs. 13 and 14. The figures contain the cell voltages and efficiencies for various fuels as a function of the fuel utilization factor.
The highest values of MCFC efficiency (50%) are obtained for methane as a fuel, just behind the ADG and LFG; syngases are characterized by lower

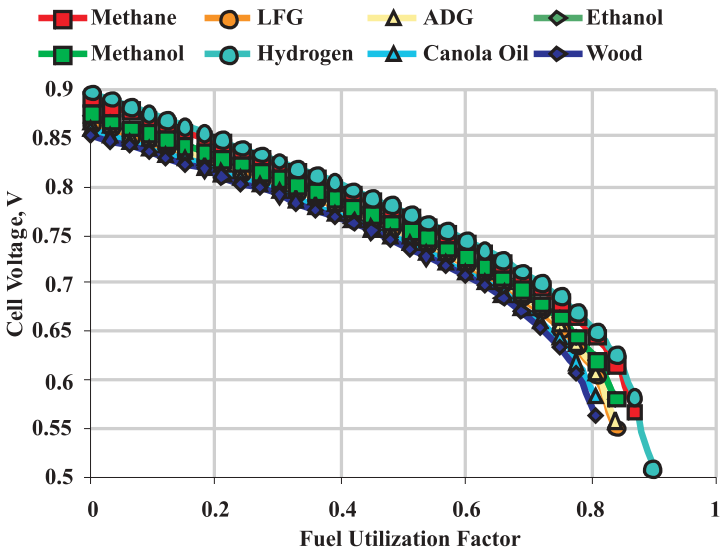

Figure 14. SOFC cell voltage vs. fuel utilization factor for various biofuels.

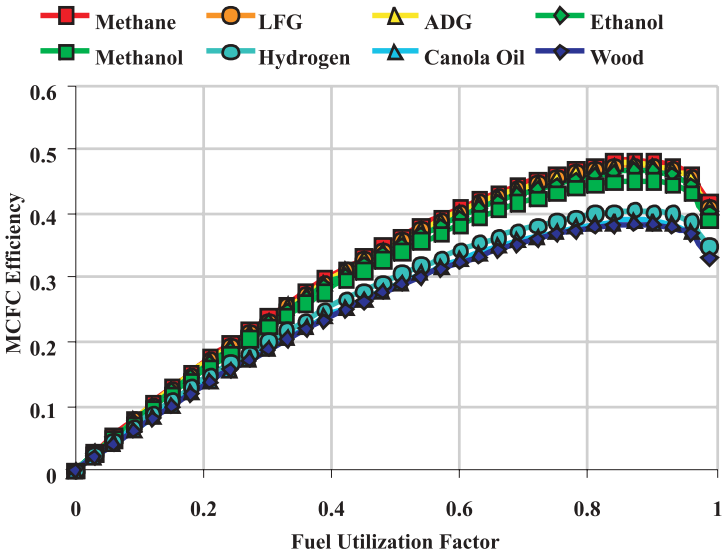

Figure 15. MCFC efficiency vs. fuel utilization factor for various biofuels.

performances (40%). The optimum values of the fuel utilization factor are very similar for all analyzed fuels.

Models were made of a molten carbonate fuel cell and a biomass fuelled

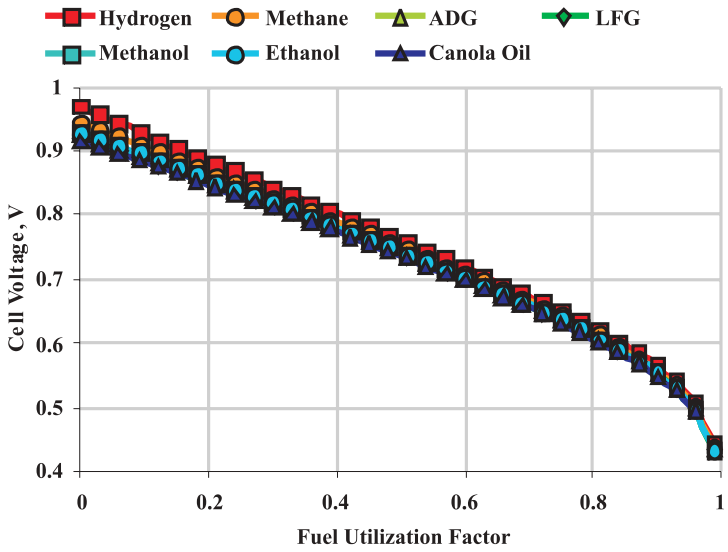

Figure 16. MCFC cell voltage vs. fuel utilization factor for various biofuels.

gasifier. The MCFC characteristics for various biofuels were obtained and commented. The presented analysis regards a design-point model in which the fuel utilization factor represents the fuel cell load. It should be noted that the same fuel utilization factor can be obtained for various cell areas, which can additionally influence cell performances. Generally speaking, biofuels are characterized by lower efficiency compared to methane. The MCFC fuelled by LFG, ADG, and alcohols outperforms both canola oil and wood. The highest open circuit voltage is achieved with hydrogen, but that does not automatically translate into greatest efficiency for higher fuel utilization factors. Internal reforming of methane means chemical conversion of process heat into a fuel (hydrogen and carbon monoxide), which achieves higher MCFC efficiency than is the case with dry hydrogen.

5 Technical and economic issues

Cash flow forecasting is a key element in determining the feasibility of investment. The main costs involved in power plant projects are up-front outlays and primary fuel supplies. Revenues take the form of proceeds from sale of electricity and heat. All those elements rely heavily on project-specific conditions. This paper also presents a simplified feasibility analysis

of fuel cells powered by biofuel. To provide a comparison, other concepts were also analyzed: reciprocating engine technology and methane fuel. The use of traditional devices – reciprocating engines being the most popular of which – can be seen as an alternative to using fuel cells for biofuel energy conversion. An alternative for biofuel can be found in traditional fossil fuel, utilized either in fuel cells or traditional devices. Presented study allows for the assumption that those types of cells can be fuelled with bioethanol. Table 7 presents efficiency values for SOFC and MCFC types for various fuels.

Table 7. Comparison of maximum efficiency values for MCFC and SOFC type cells with various fuels [%].

Fuel	Fuel cell type			
	MCFC		SOFC	
	Total	Electrical	Total	Electrical
Bioethanol	90	46.7	90	47.2
Methane	90	48.3	90	50.2

Biofuel is a loose term which includes many types of substances. Fuel cells can utilize liquid or gas fuels. Some fuels, like biogas, are generated and consumed only locally (production and combustion at the same site). Another example of a biofuel is a gasification product. There is no market as such for those fuels and this makes any reliable evaluation of their prices impossible. On the other hand, many liquid fuels are generally traded and it is possible to estimate their purchase costs. Bioethanol was selected as an example. Methane was selected as a traditional fossil alternative. A comparison of the properties of those fuels is presented in Tab. 8, 9, 10 and 12. For comparison, the possibility of utilizing those fuels in a conventional device – a reciprocating internal combustion engine – was analyzed too. Table 7 presents assumed efficiency values. Reciprocating engines cannot by fuelled by bioethanol. An efficiency decrease by 2% was assumed for bio-ethanol.

The analyzed cases concerned a combined heat and power (CHP) plant with an installed capacity of some 300–500 kW. The assumed annual equivalent full-power working time was 4500 h. All the electricity produced was to be used for the site's own consumption (the electricity price constituted the avoided purchase cost). The prices used were valid for the Polish market. The specific avoided cost for electricity purchases was 88 EURO/MWh

Table 8. Comparison of specific investment costs for discussed power plants.

Plant type	Fuel	Total investment cost, EURO/kW	Operation and maintenance cost
Reciprocating engine	Methane	1 400	0.010 EURO/kWh
	Bioethanol	1 500	0.010 EURO/kWh
SOFC	Methane	3 500	84 USD/kW/yr
	Bioethanol	3 500	84 USD/kW/yr
MCFC	Methane	2 800	96 USD/kW/yr
	Bioethanol	2 800	96 USD/kW/yr

Table 9. Main parameters of reciprocating engines [%].

Fuel	Total	Electrical
Bioethanol	93	37
Methane	93	39

– this is the average electricity purchase price for business customers according to [14]. The analysis also included revenues from renewable energy certificates in accordance with Polish regulations. The value of those was assumed to be 57.7 EURO/MWh. A similar scheme of consumption was used for heat. The assumed price of heat was 8.1 EURO/GJ.

Cash flows were calculated according to the free cash flow for the firm (FCFF) formula. Therefore no financial costs were included. Table 10 presents the net preset value (NPV) values calculated for 15 years for three types of analyzed plants: SOFC, MCFC and reciprocating internal combustion engine (ICE) and two types of fuel: methane or bioethanol. The value of NPV during the period of financial analysis is shown in Fig. 17. The results indicate that it is not feasible to use bioethanol as a fuel.

Table 10. Comparison of calculated NPV values in thousands EURO.

Plant type	Fuel type	
	Methane	Ethanol
SOFC	-291	-3 542
MCFC	-151	-3 439
ICE	182	-3 513

Therefore the next step was to calculate what level of subsidies would be

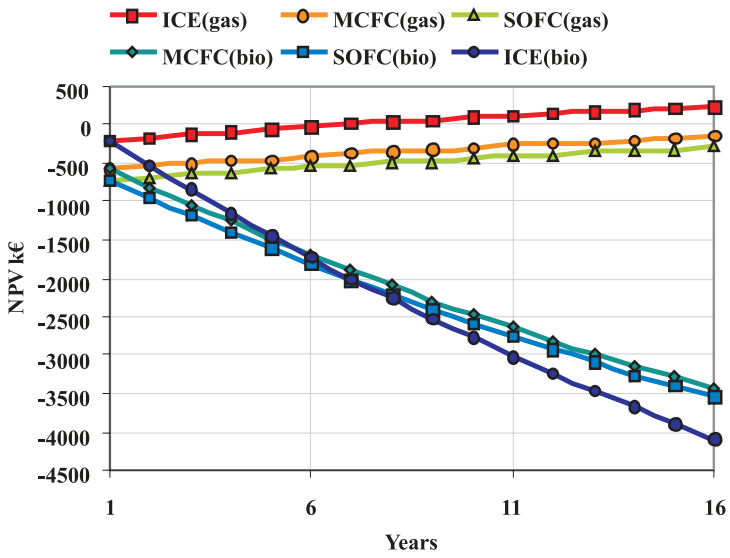

Figure 17. Net preset value changes for considered period of time.

required for bio-ethanol-based electricity generation or biofuel price to guarantee profitability (NPV=0). The results are presented in Tabs. 11 and 13.

Table 11. Comparison of subsidies for renewable electricity generation – current and required for NPV= 0 condition EURO/MWh.

Plant type	Current subsidy	Subsidy for NPV= 0
SOFC	57.7	289.2
MCFC		281.4
ICE		321,4

Table 12. Main parameters of discussed fuels.

Property	Bioethanol	Methane
Density at 15 °C	790 kg/m^3	422.62 kg/m^3
Heating value	19.59 MJ/dm^3	34.4 MJ/m^3
Price	0.86 EURO/dm^3	Tariff
	43.9 EURO/GJ	9 EURO/GJ

Table 13. Comparison of specific fuel purchase cost – current and required for NPV=0 condition.

Plant type	Current specific cost (EURO/GJ)	Specific cost for NPV=0 (EURO/GJ)
SOFC	43.9	13.5
MCFC		14.9
ICE		16.8

6 Conclusions

Models were made of a solid oxide fuel cell, a molten carbonate fuel cell and a biomass fuelled gasifier. The high temperature fuel cell characteristics for various bio-fuels were obtained and commented. The presented analysis regards a design-point model in which the fuel utilization factor represents the fuel cell load. It should be noted that the same fuel utilization factor can be obtained for various cell areas, which can additionally influence cell performances.

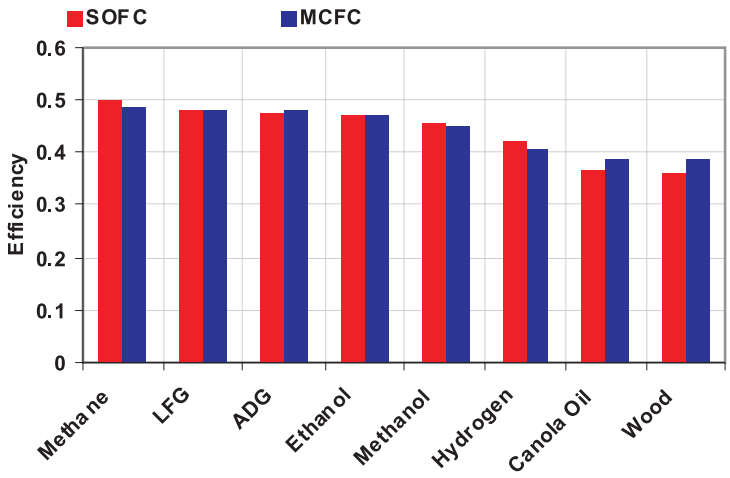

Figure 18. Maximum cell efficiency of high temperature fuel cells for various biofuels.

Generally speaking, biofuels are characterized by lower efficiency and a lower optimum fuel utilization factor than methane. The SOFC fuelled by LFG, ADG, and alcohols outperforms both canola oil and wood. The highest open circuit voltage is achieved with hydrogen, but that does not

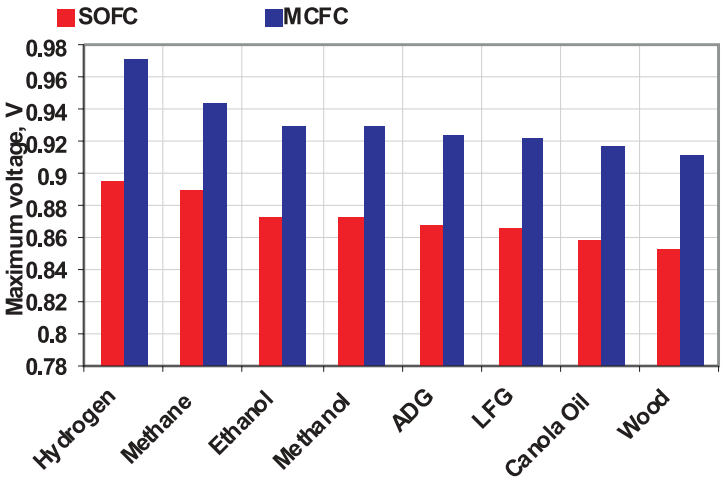

Figure 19. Maximum voltage of high temperature fuel cell for various biofuels.

automatically translate into greatest efficiency for higher fuel utilization factors. Internal reforming of methane means chemical conversion of process heat into a fuel (hydrogen), which achieves higher fuel cell efficiency than is the case with dry hydrogen. Lower working temperatures of the MCFC means higher maximum voltages than for the SOFC, but it does not translate into higher efficiencies.

Any comparison of fuel cells and ICE is problematic. Ethanol (bioethanol) is not a preferred fuel for ICE. Oil (biooil) is a better fuel for ICE, but it is impossible to use it directly in fuel cells. Bioethanol has been chosen because it can be used in fuel cells and in ICE (albeit requiring some modification of the engine and/or mixing with additional substances). Under current conditions, biofuel combustion is not feasible for either fuel cell-based plants or conventional plants (such as reciprocating engines). The level of subsidies available to promote this type of fuel is insufficient. It can be seen however that fuel cell technology would require a smaller fuel price drop or subsidy increase to provide profitability than would traditional engines. It is also pertinent to highlight the possibility of a significant drop in the investment cost for a fuel cell plant when fuel cell technology reaches the industrial production phase.

Received 10 January 2011

References

[1] Brett D.J.L. Atkinson A. Gumming A.A.D. Ramirez-Cabrera E. Rudkin R. Brandon N.P.: *Methanol as a direct fuel in intermediate temperature (500–600°C) solid oxide fuel cells with copper based anodes*. Chem.l Eng. Sci. **60**(2005).

[2] Kee R.J., Zhu H., Goodwin D.G.: *Solid-oxide fuel cells with hydrocarbon fuels*. In: Proc. of the Combustion Institute **30**, 2005.

[3] Fiyda L. Panopoulos K.D. Kakaras E.: *Integrated CHP with autothermal biomass gasification and SOFC-MGT*. Energ. Conver. and Manage. **49**(2008).

[4] Van Herle J. Maréchal F. Leuenberger S. Membrez Y. Bucheli O. Favrat D.: *Process flow model of solid oxide fuel cell system supplied with sewage biogas*. J. Power Sources **131**(2004).

[5] Assabumrungrata S., Laosiripojanab N., Pavarajarna V., Sangtongkitcharoena W., Tangjitmateea A., Praserthdama P.: *Thermodynamic analysis of carbon formation in a solid oxide fuel cell with a direct internal reformer fuelled by methanol*. J. Power Sources **139**(2005), 1-2, 55–60.

[6] Rabenstein G., Hacker V.: *Hydrogen for fuel cells from ethanol by steam-reforming, partial-oxidation and combined auto-thermal reforming: A thermodynamic analysis*. J. Power Sources **185**(2008), 1293.

[7] Milewski J., Miller A.: *Influences of the type and thickness of electrolyte on solid oxide fuel cell hybrid system performance*. J. Fuel Cell Sci. Techn. **3**(2006).

[8] *Hyprotech Corporation, HYSYS.Plant 2.1 user guide*.

[9] Jiang Y., Virkar A.V.: *Fuel composition and dilutent effect on gas transport and performance of anode supported SOFCs*. J. Electrochem. Soc. **150**(2003).

[10] Feng Z., Virkar A.V.: *Dependence of polarization in anode supported solid oxide fuel cells on various cell parameters*. J. Power Sources **141**(2005).

[11] Morita H., Komoda M., Mugikura Y., Izaki Y., Watanabe T., Maruda Y., Matsuyama T.: *Performance analysis of molten carbonate fuel cell using a Li/Na electrolyte*. J. Power Sources **112**(2002).

[12] Arato E., Bosio B., Costa P., Parodi F.: *Preliminary experimental and theoretical analysis of limit performance of molten carbonate fuel cells*. J. Power Sources **102**(2001).

[13] Milewski J., Lewandowski J.: *High temperature fuel cells fuelled by biofuels*. In: Proc. of European Fuel Cell Technology & Applications – Piero Lunghi Conference.

[14] http://epp.eurostat.ec.europa.eu

[15] Milewski J., Świrski K., Santarelli M., Leone P. Milewski J. (Eds.) *Advanced Methods of Solid Oxide Fuel Cell Modeling*. Springer-Verlag London Ltd., 2011.

[16] Milewski J.: *Advanced model of solid oxide fuel cell fuel cell science*. Engineering and Technology Conf., 2010.

[17] Milewski J. *Mathematical model of SOFC for complex fuel compositions*. Int. Colloq. on Environmentally Preferred Advanced Power Generation, 2010

[18] Milewski J.: *Modeling the influence of fuel composition on solid oxide fuel cell by using the advanced mathematical model*. Rynek Energii, **88**(2010), 159–163.

[19] Milewski J.: *Simultaneously modeling the influence of thermal-flow and architecture parameters on solid oxide fuel cell voltage ASME Fuel Cell*. Sci. and Technol., 2010

[20] Milewski J.: *SOFC hybrid system optimization using an advanced model of fuel cell*. In: Proc. 2011 Mechanical Engineering Annual Conf. on Sustainable Research and Innovation, 2011, 121–129.